UCRL-JC-132349
PREPRINT

Deformation Mechanisms in Crystalline Solids and Newtonian Viscous Behavior

O. D. Sherby, O. A. Ruano, J. Wadsworth

This paper was prepared for submittal to the
The Minerals, Metals and Materials Society (TMS) 1999 Annual Meeting
San Diego, CA
February 28-March 4, 1999

November 4, 1998

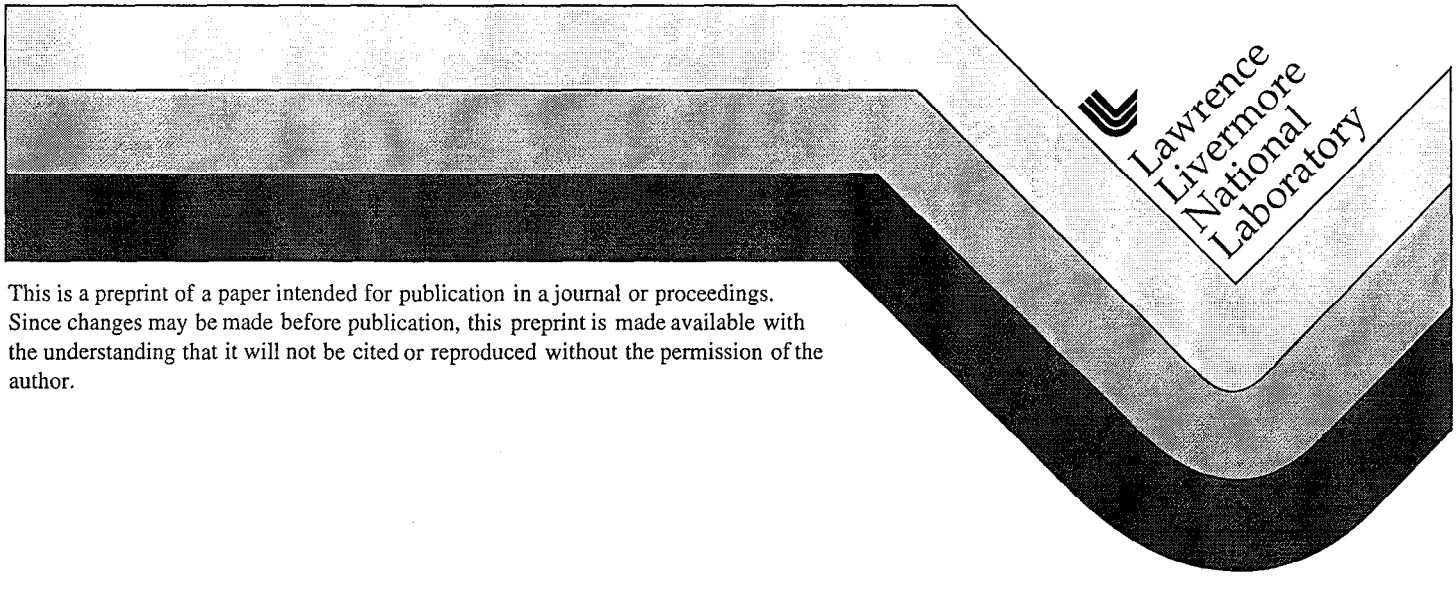

DEFORMATION MECHANISMS IN CRYSTALLINE SOLIDS AND NEWTONIAN VISCOUS BEHAVIOR

Oleg D. Sherby*, Oscar A. Ruano**, and Jeffrey Wadsworth***

*Department of Materials Science and Engineering
Stanford University
Stanford, CA 94305, USA

**Department of Physical Metallurgy, CENIM, CSIC
Avenida de Gregorio del Amo, 8
28040, Madrid, Spain

***Lawrence Livermore National Laboratory
P.O. Box 808, L-001
Livermore, CA 94550, USA

Abstract

The three principal mechanisms of plastic flow in crystalline solids at elevated temperature are crystal slip, grain boundary sliding, and diffusional flow. All three mechanisms involve the diffusion of atoms as the rate-controlling process, either in the lattice or in the grain boundary. Under the correct conditions of microstructure, temperature, and stress, each mechanism can lead to Newtonian-viscous behavior. That is, the strain rate increases linearly with the applied stress. In the case of crystal slip, Newtonian-viscous behavior is observed at very low stresses and, in pure metals, is known as Harper-Dorn (H-D) creep. This Newtonian behavior can also be observed in anisotropic crystalline solids that are deformed under thermal cycling conditions. The dislocation density and the stacking fault energy are important structural factors that contribute to crystal slip-controlled Newtonian flow. In the case of grain boundary sliding, Newtonian-viscous behavior is observed in fine-grained, solid solution alloys under conditions where grain-boundary sliding is accommodated by dislocation glide controlled by the diffusion of solute atoms. In the case of diffusional creep, which is rigorously described by the Nabarro-Herring (N-H) theory, the creep rate is controlled by grain size and by the rate of atom diffusion in the lattice and in the grain boundary. Deformation mechanism maps describe the conditions of dislocation density, grain size, stress, and temperature under which each deformation process can be expected to be rate-controlling.

Historical Perspective

Plastic flow in crystalline solids, and in particular metallic polycrystals, is normally non-Newtonian. That is, the flow stress-strain rate relation is generally not linear; rather, the flow rate increases exponentially with stress. There are a number of examples, however, where Newtonian-viscous behavior is in fact observed.

The first evidence for such behavior was by Chalmers, in 1937, who studied the creep of tin single crystals at room temperature and at low stresses (1). Chalmers showed the creep rate to be constant over a small strain, in the order of 10^{-6} to 10^{-5}, and also discovered that the creep rate increased linearly with the stress. This behavior was named "microcreep" because it was observed only at small strains. Chalmers related these results to the motion of dislocations (dislocation theory had been introduced just three years earlier) but did not attempt to develop a specific model. Chalmers' work created quite a stir among metal plasticians. This was because an example had been found in metallic solids that could be related to the Newtonian flow of liquids, in which diffusion of atoms was known to be the rate-controlling process.

In 1941, Kauzmann developed a creep relation based on Eyring's thermally-activated, reaction-rate, theory (2), which supported Chalmers' results. Using dislocations as the source of slip, with an activation energy that was influenced by stress, Kauzmann obtained a hyperbolic sine relation for creep. This theory predicted Newtonian-viscous flow at low stresses and an exponential dependence with stress at high stresses. The theory, however, did not allow a quantitative prediction of the actual creep rate at a given stress.

In 1948, Nabarro pointed out the inadequacies of the Kauzmann model (3). In addition, he attempted to relate the creep of tin to his diffusional creep model but concluded that his theory could not explain the limiting strain observed for the "microcreep" process.

After the publications of Chalmers and Nabarro, the next evidence for Newtonian flow came from low-stress creep data of polycrystals tested near the melting temperature. These results were found for polycrystalline copper, in 1949, by Udin, Shaler, and Wulff (4) and for polycrystalline gold, in 1951, by Alexander, Dawson, and Kling (5). These data have been interpreted as evidence for the diffusional creep process of Nabarro and Herring.

In 1957, Harper and Dorn (6) studied the creep of polycrystalline aluminum near its melting temperature and showed Newtonian flow behavior. The observed creep rates, however, were shown to be higher than those predicted by the diffusional creep process. Because of this discrepancy, attempts were made to suggest that it was the subgrain boundaries present within the grains, rather than the grains, that could be the sources of sinks and vacancies. In this way, the predicted creep rate from the Nabarro-Herring theory could then be rationalized with the Harper and Dorn results. This has been proven to not be the mechanism, and it is now generally accepted that Harper-Dorn creep is an independent mechanism based on a diffusion-controlled, dislocation creep, process. In 1984, Wu and Sherby (7) showed that Chalmers' microcreep data are in agreement with this Harper-Dorn creep mechanism.

The discussion thus far has been confined to Newtonian-viscous flow in crystalline solids obtained under isothermal conditions. Newtonian-viscous flow can also occur when certain metallic materials are deformed under thermal cycling conditions. Perhaps the first investigator on this finding was Sauveur (8); in 1924, he showed that iron became extremely weak when creep tested under phase transformation conditions (alpha to gamma and back to alpha). Koref

(9), in 1926, and Schiel (10), in 1932, used the term "amorphous plasticity" to described this type of plasticity, thus relating it to a Newtonian-viscous, liquid-like, behavior.

A mechanical model to interpret transformation plasticity was given by Greenwood and Johnson (11) in 1965. Subsequently, Lobb, Sykes, and Johnson (12), in 1972, showed Newtonian-viscous flow occurred in zinc and alpha uranium when creep tested under thermal cycling conditions where no phase transformations occur. These results are related to the development of internal stresses arising from crystal anisotropy of the thermal expansion coefficients in these non-cubic structure metals.

Research on thermal cycling of fiber-and-particle-reinforced aluminum composites revealed similar Newtonian-viscous behavior (13). In this case, the internal stress is created from differences in the thermal expansion coefficients of the non-metallic reinforcing material and the aluminum matrix. An internal stress (superplasticity) model was developed by Wu, Wadsworth, and Sherby (14) in 1987. The model gave predictions which were in quantitative agreement with experimental data for zinc, uranium, and aluminum matrix composites.

Grain boundary sliding in fine-grain materials can lead to Newtonian-viscous flow. Fukuyo et al (15), in 1991, showed that Class I solid solution alloys containing fine grains exhibited Newtonian-viscous flow. In these cases, the rate-controlling process was grain boundary sliding accommodated by solute drag dislocation glide.

Examples for Newtonian-Viscous Flow in Crystalline Solids

The following examples are shown, in the order of historical perspective, for each of the four categories of Newtonian-viscous flow described above. These are Harper-Dorn creep, Nabarro-Herring diffusional creep, internal-stress-assisted (superplastic) creep, and grain boundary sliding creep.

1. Harper-Dorn creep

Figure 1 shows creep data for pure aluminum plotted as lattice-diffusion-compensated, steady state creep rate as a function of the modulus-compensated stress. The Harper-Dorn viscous-creep region is observed at low stresses where the stress exponent is unity. At high stresses power-law creep is observed where the stress exponent is five. The solid line in the figure is the predicted curve from an internal stress-assisted dislocation creep model (16). This model is based on the assumption that moving dislocations are envisioned to be both aided and inhibited by the presence of internal stress fields that arise from stationary dislocations. Specifically, it was proposed that, at any given moment, one half of the moving dislocations are influenced by an internal stress that adds to the applied stress, and the remaining half of the moving dislocations are influenced by an internal stress that subtracts from the applied stress. In equation form, the steady state creep rate, $\dot{\varepsilon}$, as a function of the applied stress, σ, is described as follows:

$$\dot{\varepsilon} = \frac{1}{2} A_{PL} \frac{D_{eff}}{b^2} \left\{ \left(\frac{\sigma+\sigma_i}{E} \right)^n + \frac{|\sigma-\sigma_i|}{(\sigma-\sigma_i)} \cdot \left| \frac{\sigma-\sigma_i}{E} \right|^n \right\} \qquad (1)$$

In this equation, A_{PL} is a material constant that describes power law creep, b is the burgers vector, n is the exponent for power-law creep (n=5), E is the dynamic, average, unrelaxed,

polycrystalline, Young's modulus, D_{eff} is the effective diffusion coefficient which incorporates contributions from both lattice and dislocation pipe diffusion, and σ_i is the internal stress.

At low stresses, where $\sigma < \sigma_i$, equation (1) reduces to the Harper-Dorn, Newtonian-viscous, creep relation:

$$\dot{\varepsilon} = A_{PL} \cdot n \frac{D_{eff}}{b^2} \left(\frac{\sigma_i}{E}\right)^{n-1} \frac{\sigma}{E} \tag{2}$$

At high stresses, where $\sigma >> \sigma_i$, equation (1) reduces to the power- law creep relation:

$$\dot{\varepsilon} = A_{PL} \frac{D_{eff}}{b^2} \left(\frac{\sigma}{E}\right)^{n} \tag{3}$$

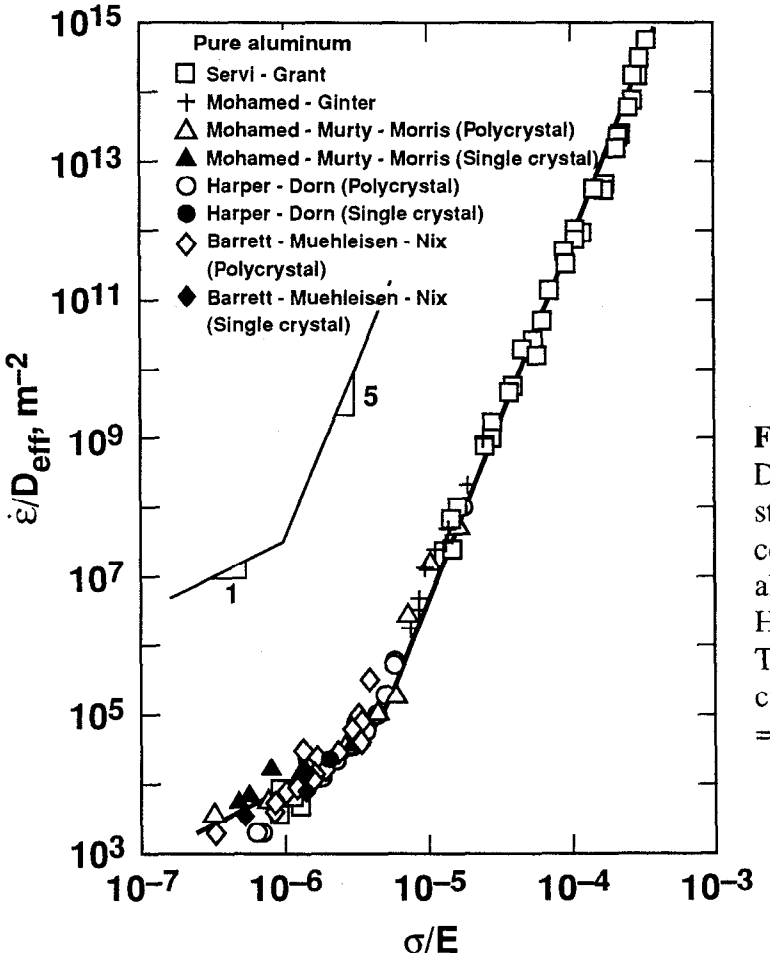

Figure 1.
Diffusion-compensated-steady-state-creep rate vs. modulus-compensated stress data for pure aluminum in the power law and Harper—Dorn creep regimes. The solid line is the predicted curve from equation (1) with $\sigma_i/E = 2.5 \times 10^{-6}$. (16)

The value of the modulus-compensated internal stress for pure aluminum, to make the good fit shown in Fig. 1, is:

$$\frac{\sigma_i}{E} = 2.5 \cdot 10^{-6} \tag{4}$$

This value of internal stress has been shown to be related to the dislocation density that is predicted from the Taylor equation for plastic yielding in crystals. Figure 2 shows a plot of the modulus-compensated internal stress as a function of dislocation density, ρ, for aluminum and alpha zirconium. These are the only two metals where σ_i/E and ρ have been measured. The data fall close to the predicted line given by the Taylor equation, and give strong support for the internal stress-assisted model described by equation (1). A number of alternative creep models

for Harper-Dorn creep have been proposed (17-22). The correct model requires taking into account a number of factors that influence Harper-Dorn creep. These are dislocation density and substructure, stacking fault energy, solute atom-dislocation interactions, grain size, particle size and distribution, and atom mobility. An example of the complexity of Harper-Dorn creep is the influence of annealing or soaking time at high temperature on the creep rate in the Newtonian-viscous regime (23,24) which is not yet resolved.

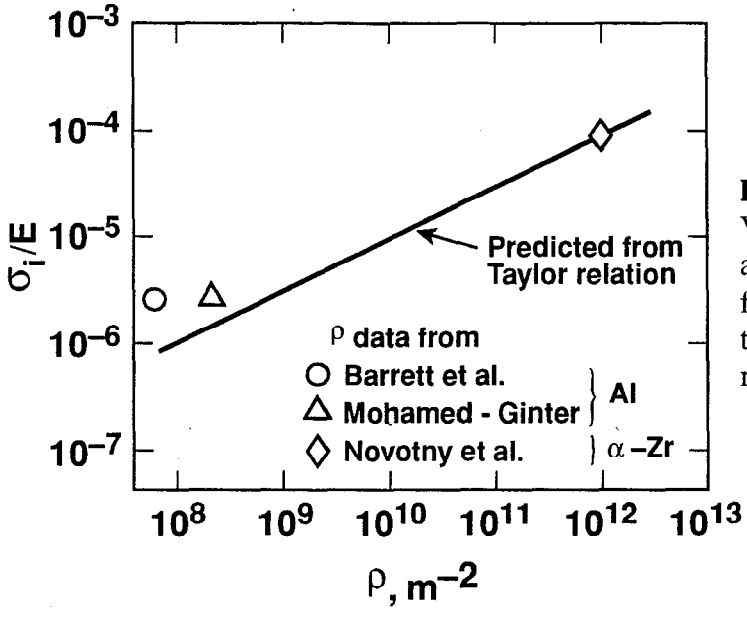

Figure 2.
Values of σ_i/E from creep data as a function of dislocation density for Al and α–Zr, compared with the prediction from the Taylor relation. (16)

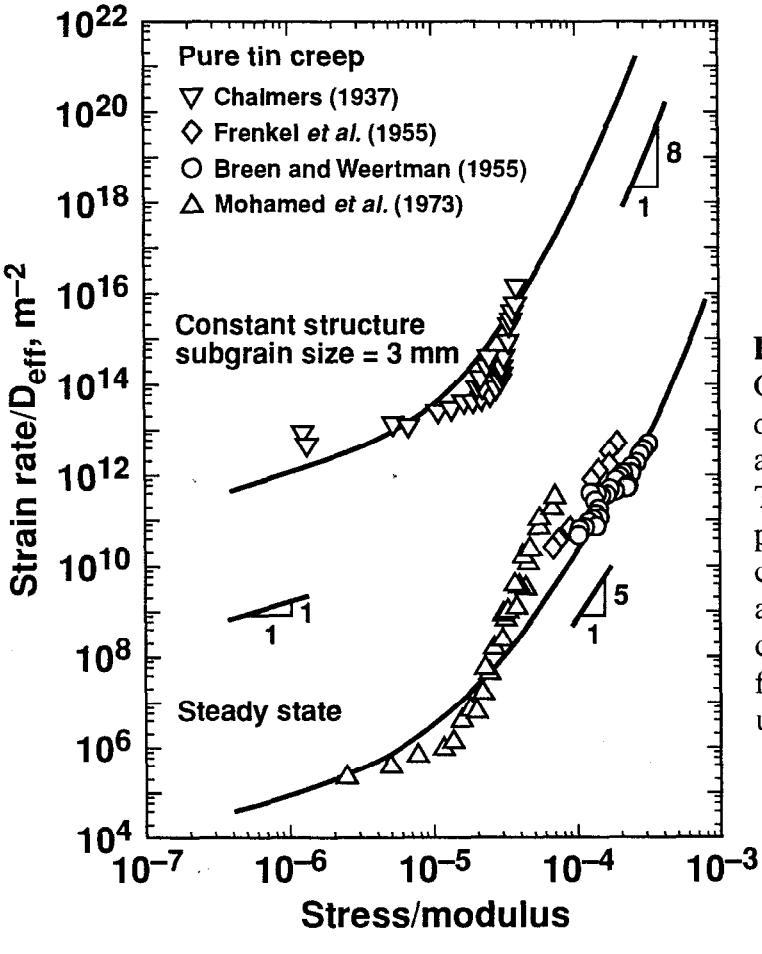

Figure 3.
Comparison of the micro-creep data of Chalmers for pure tin with a constant structure creep relation. The steady state creep data for pure tin is included for comparison. All data are plotted as effective-diffusivity-compensated strain rate as a function of modulus-compensated uniaxial stress. (7)

The "microcreep" tin data of Chalmers described earlier has been explained by the internal-stress-assisted model (7,14). The "microcreep" data (obtained at 0.57 Tm) and the low stress creep data of Mohamed et al (obtained at 0.99 Tm) are plotted in Fig. 3. The two sets of data are widely separated although Newtonian-viscous behavior is observed at low stresses for both investigations. The difference in the two data groups is attributed to dislocation density differences as well as to differences in dislocation barrier spacing (7,14).

2. Nabarro-Herring diffusional creep

The schematic model of Nabarro for developing the diffusional creep theory is illustrated in Fig. 4. The stress state shown leads to a vacancy gradient from the boundaries in tension to the boundaries in compression. The initial dimensions of the sample are given by RSTU. Atoms at X and Y move in opposite directions under stress *P*. This directional migration of vacancies under stress leads to a change in shape of the original material. The model leads to the following relation:

$$\dot{\varepsilon} = \frac{14 D_L b^3 \sigma}{d^2 kT} \qquad (5)$$

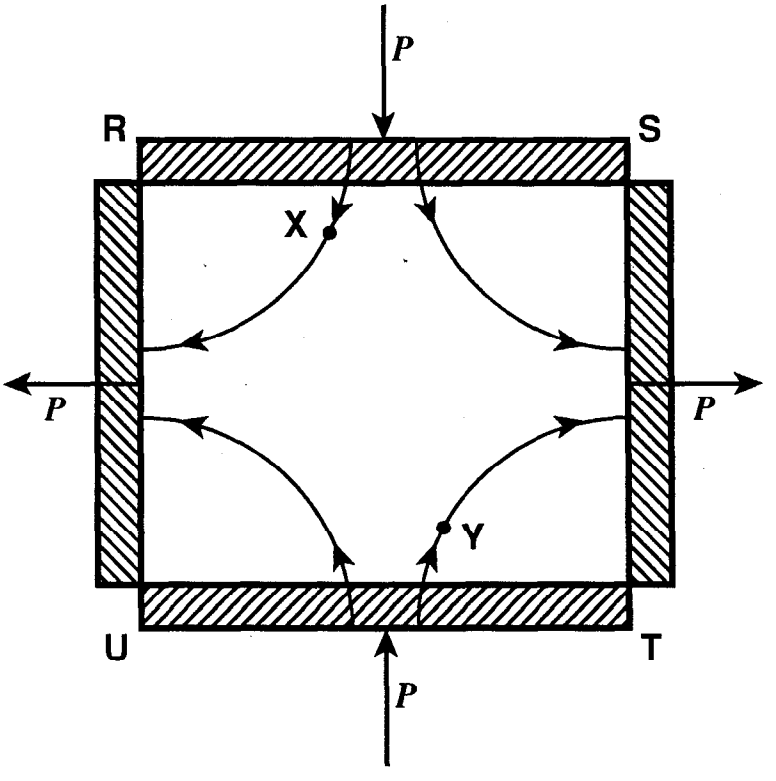

Figure 4.
A block of metal under shear stress *P*. If the block creeps under the stress, atoms at X and at Y move in opposite directions (after Nabarro). (3)

In this relation, d is the true grain size and k is the Boltzmann constant. This Nabarro model was refined mathematically, although quantitatively unchanged, by Herring (25) in 1950. The possible evidence for diffusional creep came soon after the theory was developed from low stress creep tests focused on measuring surface and grain boundary energies. These studies were with copper (4) and gold (5). These low stress creep results are compared with a number of other pure metals in Fig. 5 (26). As can be seen, the copper and gold data fall on the predicted line. All the other metals fall above the predicted line showing power law creep. Later, creep data at low stresses on a number of metals, where Newtonian-viscous flow was observed, were initially interpreted to be evidence of diffusional creep (27). An alternative

view, however, was presented indicating that Harper-Dorn creep was more likely to be the rate-controlling process in these new studies (16), with one exception, i.e., delta iron. In the case of copper, the data shown in Fig. 5, together with other data on low stress creep of copper, indicated that Harper-Dorn creep is the dominant process at low stresses (23).

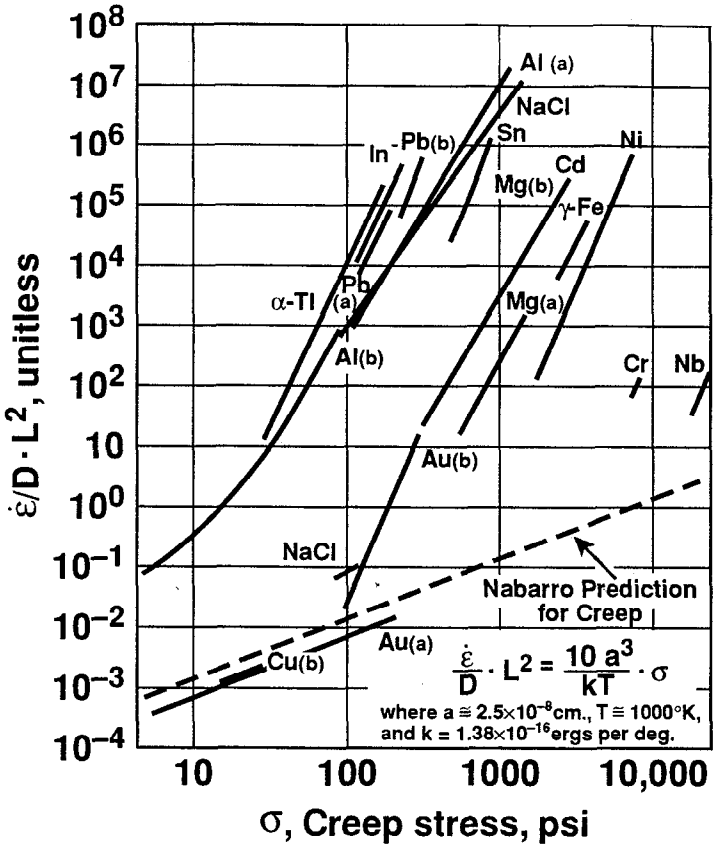

Figure 5.
Comparison of creep behavior of various pure polycrystalline metals with Nabarro—Herring diffusional creep theory. Cu and Au appear to agree with the Nabarro—Herring prediction at low stresses but Al does not. (26)

Newtonian-viscous flow has been observed at low stresses at intermediate temperatures. These data have been interpreted as diffusional creep but with grain boundary diffusion as the rate-controlling process. Coble was the first to suggest this process, in 1963; the mechanism is now known as Coble diffusional creep (28). It has been shown, however, that these intermediate stress data are best explained by either Harper-Dorn creep or grain boundary sliding (24).

3. Internal-stress-assisted (superplastic) creep

Thermal cycling during creep of many metal-base alloys can lead to Newtonian-viscous flow. An example is that of 6061 aluminum containing 20% SiC whiskers. Newtonian-viscous flow leads to ideal superplastic behavior and high elongations are achieved. An example is shown in Fig. 6. Only 12% elongation is achieved in this composite when deformed isothermally at 450°C and at a strain rate of $\dot{\varepsilon} = 10^{-4}s^{-1}$. On the other hand, the same composite exhibits 1400% elongation when deformed under thermal cycling conditions, (100 ↔ 450°C at 100 seconds per cycle) under a stress of 10 MPa (29). The basis of understanding this behavior is that internal stresses are developed at the interfaces between the aluminum matrix and the SiC fibers. This is because the expansion coefficient of aluminum is six times larger than that of silicon carbide fibers. These internal stresses will relax by plastic deformation in the aluminum matrix to the value of the local interfacial yield stress of the material. It is this remaining local yield stress, which is the internal stress, σ_i, in the creep model given earlier as equation (1).

The predictive nature of the internal stress-assisted plasticity model is shown in Fig. 7 for a 2024 aluminum alloy containing 10% and 20% SiC whiskers. It is seen that the diffusion-compensated strain rate is higher for the thermally-cycled materials than for the isothermally-tested materials. Of significance is the higher rate of creep of the 20% SiC_w material compared to the 10% SiC_w material under thermal cycling conditions. This is because the internal stress, σ_i (equal to the yield strength of the composite at the interface), is higher for the 20% SiC_w material than for the 10% SiC_w material (as observed in the isothermal data). The solid lines are the predicted curves from equation (1), which agree well with the data showing Newtonian-viscous creep at low stresses for the thermally-cycled materials.

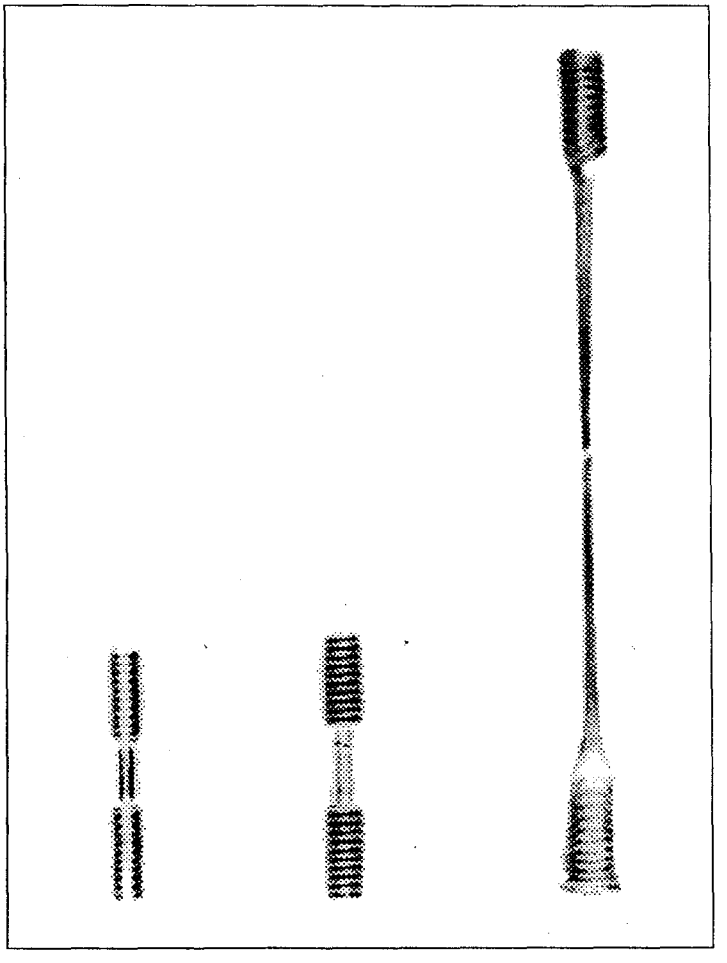

Figure 6.
Tensile ductility of Al-6061—SiC_w reinforced composite. (29)

Left: The untested condition.
Center: 12% elongation under isothermal testing at 450°C and at $\dot{\varepsilon} = 10^{-4} s^{-1}$.
Right: 1400% elongation under thermal cycling conditions (100↔450°C) at σ=10 MPa.

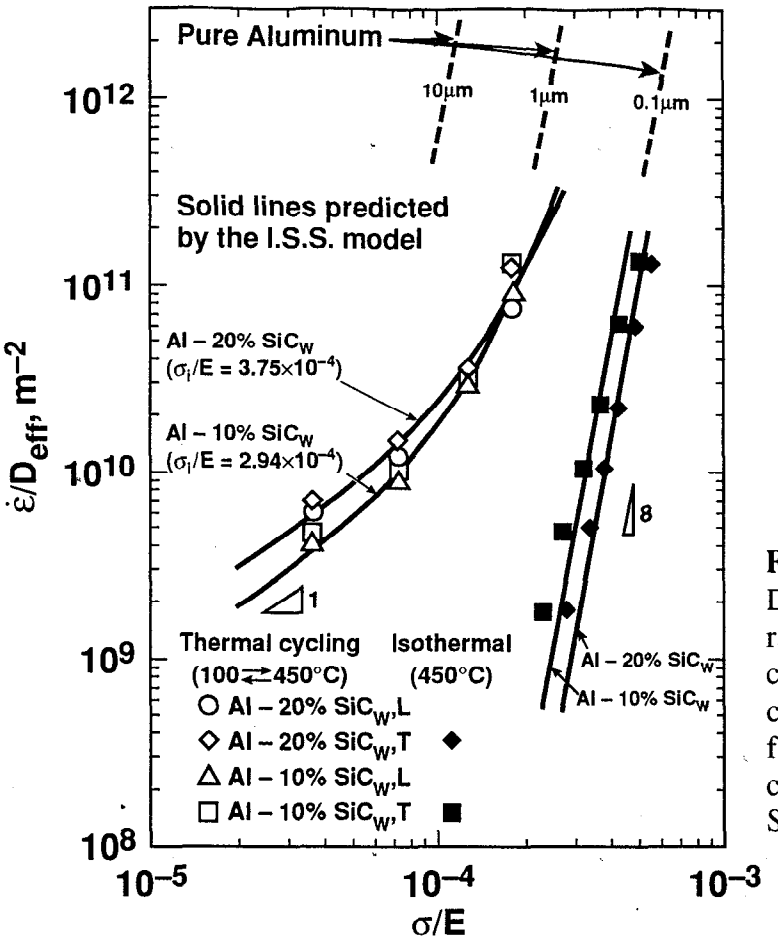

Figure 7.
Diffusion-compensated strain rate as a function of modulus-compensated stress for thermal cycled and isothermal creep data for Al-2024 alloy composite containing 10%SiC_w and 20% SiC_w. (30)

The manner in which silicon-carbide whiskers flow during plastic deformation of the aluminum composites, differs dramatically under thermal cycling condition compared to isothermal conditions (30, 31). Figure 8 shows the difference in flow behavior of an extruded 2024-20% SiC_W composite conducted in compression under isothermal and thermal cycling conditions. The sample that was deformed isothermally exhibited very limited reorientation of the whiskers. Furthermore, extensive surface cracks were observed in the sample. On the other hand, the sample that was deformed under thermal cycling conditions, to the same strain, shows that nearly all whiskers were no longer in the original longitudinal direction. Clearly, Newtonian-viscous flow of the metal matrix accelerates the reorientation of the whiskers. No surface cracks were observed in the thermally-cycled samples.

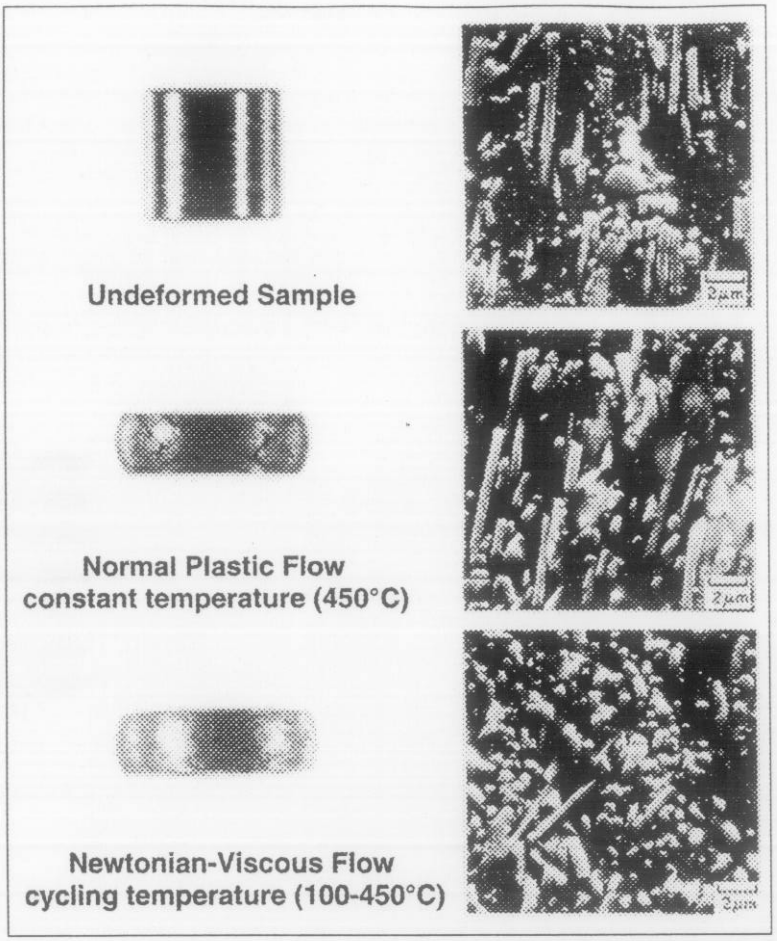

Figure 8.
Illustration that Newtonian-viscous flow in a whisker reinforced Al-2024—20% SiC_w composite leads to crack-free plastic flow and to rapid reorientation of whiskers. (31)

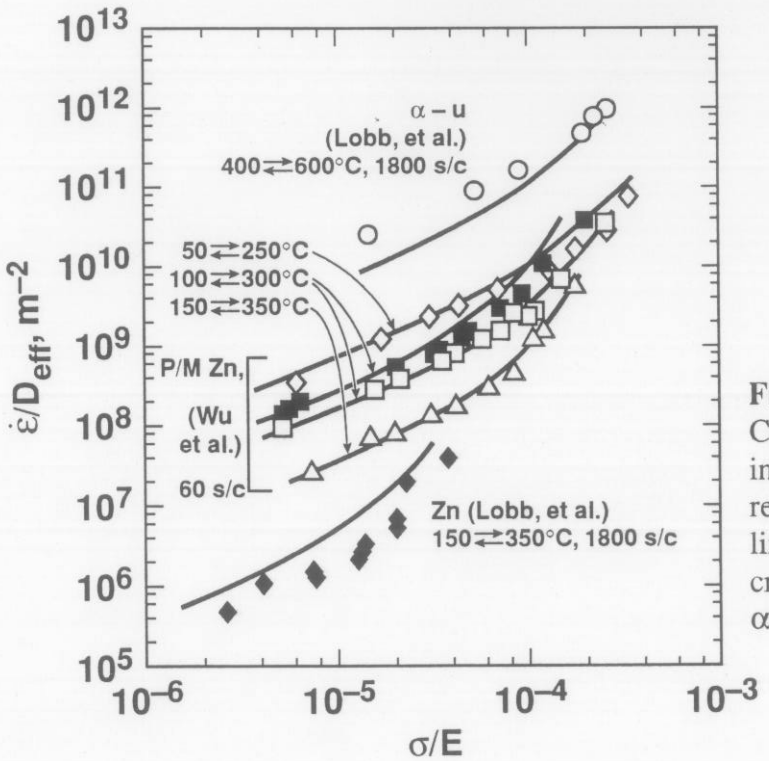

Figure 9.
Comparison of the proposed internal stress plasticity relations, given by the solid lines, with all thermal cycling creep data available for Zn and α-U. (14)

Internal-stress plasticity as modelled by equation (1) has also been applied to metals that have anisotropic thermal expansion coefficients such as hexagonal close-packed zinc and body-centered orthorhombic alpha uranium. The predicted creep behavior of these anisotropic metals is shown in Fig. 9. As can be seen, the predicted curves agree remarkably well with experimental data which include variables in the temperature range of thermal cycling (zinc tests) and in the cycling rate given as seconds per cycle (zinc versus uranium tests). At low values of the modulus-compensated stress, the model predicts, and the data demonstrate, the existence of ideal Newtonian-viscous flow (n=1); under these experimental conditions, superplastic behavior is indeed observed (12-14).

4. Grain-boundary sliding creep

It is generally accepted that grain-boundary sliding is the dominant mechanism for superplastic flow of fine-grained materials at high temperatures. The stress exponent for this mechanism is typically two, hence most superplastic materials, although highly strain-rate sensitive, do not show Newtonian-viscous behavior. The grain boundary sliding model of Ball and Hutchinson (32), however, illustrates the possibility of achieving Newtonian-viscous creep in fine-grained materials. The Ball-Hutchinson model is based on a grain boundary sliding process accommodated by slip and a schematic of the model is shown in Fig. 10.

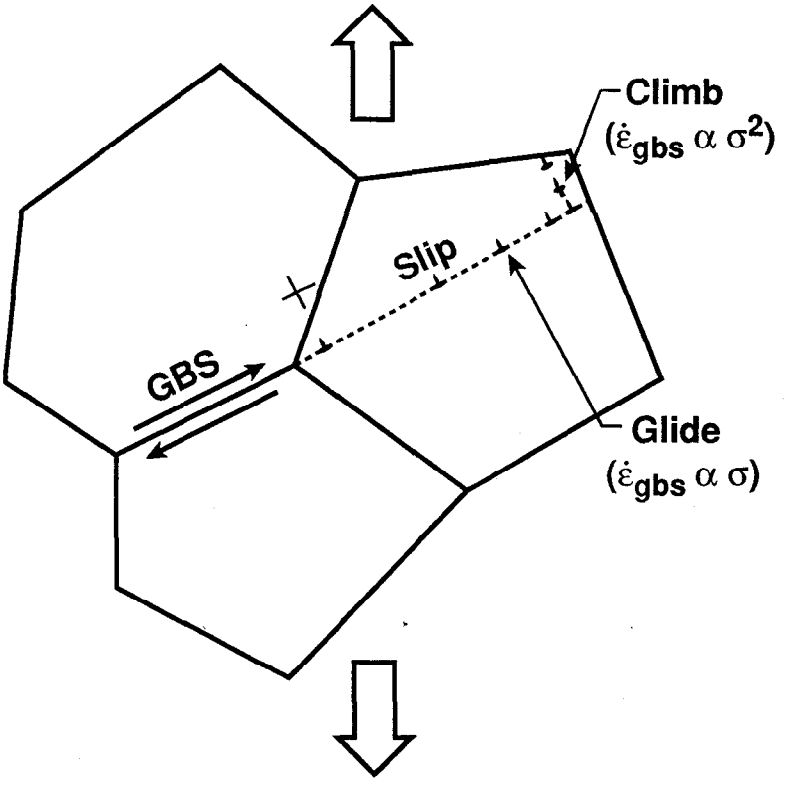

Figure 10.
Model illustrating grain boundary sliding accommodated by dislocation motion involving the sequential steps of glide and climb. (15)

As can be seen, the slip-accommodation process involves the sequence step of glide and climb of dislocations. When climb is the rate-controlling step, the strain rate sensitivity exponent is 0.5 (that is n = 2) because of the extra stress term from dislocation pile-up at the head of the climbing dislocation. This leads to the grain boundary sliding relations developed by Ball and Hutchinson, and later expanded by Langdon (33), and by Mukherjee (34). When glide is the rate-controlling processing step, however, the strain-rate-sensitivity exponent is unity because

there is no pile-up stress. Since glide and climb are sequential processes, the slower of the two processes is rate-controlling. Fukuyo et al (15) showed that this could occur in fine-grained Class I solid solution alloys since in these alloys the glide step (solute-drag controlled dislocation creep) is often the slowest process. On the other hand, fine-grained Class II solid solution alloys, where dislocation climb is the rate-controlling step, should exhibit strain-rate-sensitivity exponents equal to 0.5.

The predictions of Fukuyo et al have been confirmed for a number of fine-grained Class I solid solution alloy systems studied at high temperatures, as can be seen in Fig. 11. The strain-rate-sensitivity exponent, m, is shown as a function of strain rate. The strain rate is normalized to the strain-rate-sensitivity exponent equal to 0.3 in order to assess the different Class I solid solution alloys to a common base. Starting from the lowest strain rate tests, where m is equal to 0.5, is the range where grain-boundary-sliding accommodated by dislocation climb is rate-controlling. With an increase in strain rate, the value of m increases towards unity. This is the range where grain-boundary-sliding accommodated by solute-drag-controlled dislocation glide is rate-controlling; i.e. it becomes a slower process than dislocation climb. At yet higher stresses, slip deformation becomes the more facile process, m decreases, and if solute drag slip is rate-controlling the m values become equal to 0.33.

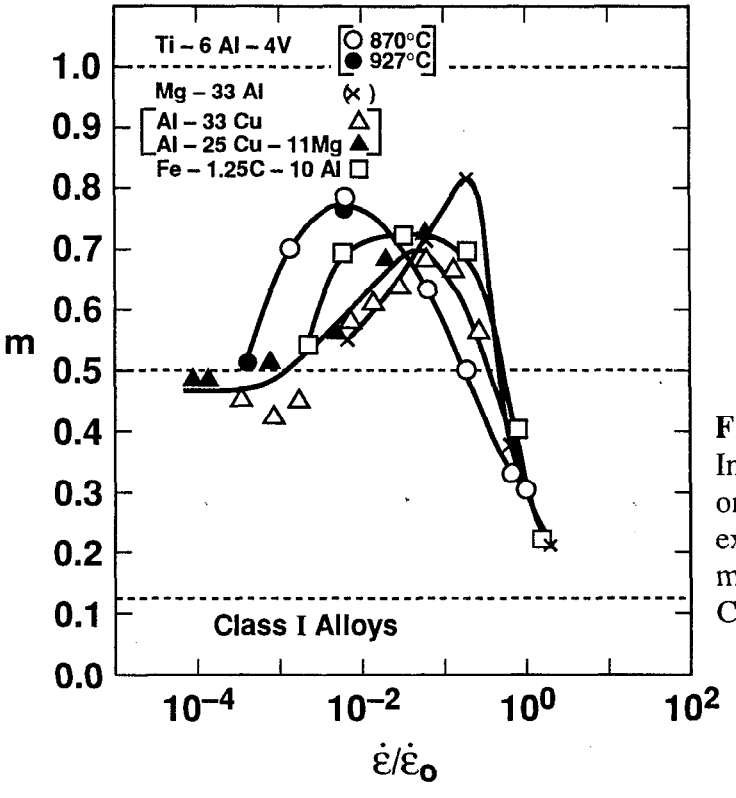

Figure 11.
Influence of normalized strain rate on the strain-rate-sensitivity exponent, m, for superplastic materials considered as fine-grained Class I solid solution alloys. (15)

Ideal Newtonian-viscous flow was found in fine-grained ultrahigh carbon steels (UHCSs) containing a large amount of aluminum following the original work of Fukuyo et al. Some of these data are shown in Fig. 12 where the flow stress is plotted as a function of strain rate for three UHCSs containing 7 to 10% aluminum (35-37). At low strain rates, the strain-rate sensitivity exponent m is equal to 1, and at high strain rates the strain-rate-sensitivity exponent m is equal to 0.33. These are in agreement with the expected behavior of fine-grained Class I solid solution alloys when slip is rate-controlling.

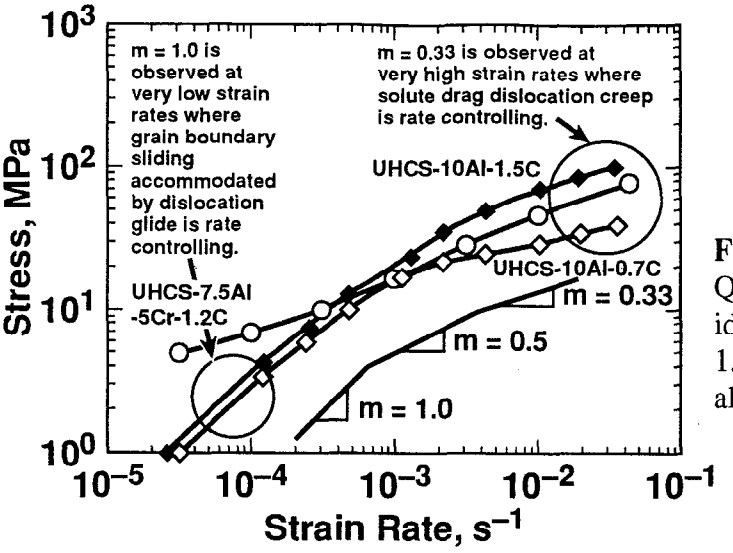

Figure 12.
Quasi-superplasticity (m = 0.33) and ideal grain-boundary sliding (m = 1.0) are observed in UHCS-high aluminum alloys. (35, 36)

Conclusions

Newtonian-viscous flow is observed in crystalline solids in all three of the deformation mechanisms controlling plastic flow, namely crystal slip, diffusional creep, and grain boundary sliding. In most cases, Newtonian-viscous behavior is only observed at low strain rates, low stresses, and high temperatures where either slip creep or diffusional creep is controlling the deformation process. Newtonian-viscous flow is obtained by the thermal cycling of anisotropically expanding materials and is controlled by an internal-stress-assisted dislocation creep process. Fine-grained Class I solid solution alloys exhibit Newtonian-viscous flow at intermediate to high temperatures that is controlled by a grain-boundary-sliding process accommodated by solute-drag dislocation glide.

Acknowledgements

This work was performed under the auspices of the U.S. Department of Energy by Lawrence Livermore National Laboratory under Contract W-7405-Eng-48.

References

1. B. Chalmers, Proc. Roy. Soc. A, 156, 427 (1937).

2. W. Kauzmann, Trans. Met. Soc., AIME, 143, 57 (1941).

3. F.R.N. Nabarro, Report of the Conference on the Strength of Solids, p75, Physical Society, London (1948).

4. H. Udin, A.J. Shaler and J. Wulff, Trans. Metall. Soc. AIME, 185, 186 (1949).

5. B.M. Alexander, M.H. Dawson, and H.P. Kling, J. Appl. Phys., 22, 439 (1951).

6. J.C. Harper and J.E. Dorn, Acta Metall., 5, 654 (1957).

7. M. Y. Wu and O.D. Sherby, Acta Metall., 32, 1561 (1984).

8. A. Sauveur, Iron Age, 113, 581 (1924).

9. F. Koref, Z. Techn. Physik, 7, 544 (1926).

10. E. Schiel, Z. Anorg. Chem., 207, 21 (1932).

11. G.W. Greenwood and R.H. Johnson, Proc. Roy. Soc. A., 283, 403 (1965).

12. R.C. Lobb, E.C. Sykes, and R.H. Johnson, Metal. Sci. J., 6, 33 (1972).

13. M.Y. Wu and O.D. Sherby, Scripta Metall., 18, 773, (1984).

14. M.Y. Wu, J. Wadsworth, and O.D. Sherby, Met. Trans. A, 18A, 451 (1987).

15. H. Fukuyo, H.C. Tsai, T. Oyama and O.D. Sherby, ISIJ Int., 31, 76 (1991).

16. O.A. Ruano, J. Wadsworth and O.D. Sherby, Acta Metall., 36, 1117 (1988).

17. F.A. Mohamed and T.G. Ginter, Acta Metall., 30, 1869 (1982).

18. T.G. Langdon and P. Yavari, Acta Metall., 30, 881 (1982).

19. J. Weertman and J. Blacic, Geophys. Res. Lett., 11, 117 (1984).

20. A.J. Ardell and S.S. Lee, Acta Metall., 34, 2411 (1986).

21. S.V. Raj, Scripta Metall., 19, 1069 (1985).

22. V. Raman and S. V. Raj, Scripta Metall., 19, 629 (1985).

23. O.A. Ruano, J. Wadsworth, J. Wolfenstine, and O.D. Sherby, Mater. Sci. Eng., A165, 133 (1993).

24. J. Wadsworth, O.A. Ruano, and O.D. Sherby, February, 1999 TMS Annual Meeting, San Diego, California, USA.

25. C. Herring, J. Appl. Phys., 21, 437 (1950).

26. O.D. Sherby and P.M. Burke, Prog. Mater. Sci., 13, 325 (1967).

27. H. Jones, Mater. Sci. Engrg., 4, 106 (1969).

28. R.L. Coble, J. Appl. Phys., 34, 1679 (1963).

29. G. Gonzalez-Doncel, S.D. Karmarkar, A.P. Divecha, and O.D. Sherby, Comp. Sci. Technol., 35, 105 (1989).

30. S.H. Hong, O.D. Sherby, A.P. Divecha, S.D. Karmarkar, and B.A. MacDonald, Inst. Comp. Mater., 22, 102 (1988).

31. M.Y. Wu and O.D. Sherby, Scripta Metall., 18, 773, (1984).

32. A. Ball and M.M. Hutchinson, Met. Sci. J., 3, 1 (1969).

33. T.G. Langdon, Phil. Mag., 22, 689 (1970).

34. A.K. Mukherjee, Mater. Sci. Eng., 8, 83 (1971).

35. H.C. Tsai, Ph.D. dissertation, 1990, Stanford University, Stanford, CA.

36. O.D. Sherby, T.G. Nieh, and J. Wadsworth, Materials Science Forum, 170-172, (Ed. T.G. Langdon), Trans. Tech. Publications, Switzerland, (1994).

37. O.D. Sherby, D.R. Lesuer, and C.K. Syn, Proceedings of the International Conference on Advanced Materials, 2, Chinese Journal of Mechanics Press, Beijing, China, 1919 (1966).